

reaction of the major human abasic endonuclease: new insights from EDTA-resistant incision of acyclic abasic site analogs and site-directed mutagenesis. *J. Mol. Biol.* **290**, 447–457 (1999).

13. Izumi, T. *et al.* Intragenic suppression of an active site mutation in the human apurinic/apyrimidinic endonuclease. *J. Mol. Biol.* **287**, 47–57 (1999).
14. Kane, C. M. & Linn, S. Purification and characterization of an apurinic/apyrimidinic endonuclease from HeLa cells. *J. Biol. Chem.* **256**, 3405–3414 (1981).
15. Masuda, Y., Bennett, R. A. & Demple, B. Dynamics of the interaction of human apurinic endonuclease (Ape1) with its substrate and product. *J. Biol. Chem.* **273**, 30352–30359 (1998).
16. Bennett, R. A. O., Wilson, D. M., Wong, D. & Demple, B. Interaction of human apurinic endonuclease and DNA polymerase β in the base excision repair pathway. *Proc. Natl Acad. Sci. USA* **94**, 7166–7169 (1997).
17. Prasad, R. *et al.* Specific interaction of DNA polymerase β and DNA ligase I in a multiprotein base excision repair complex from bovine testis. *J. Biol. Chem.* **271**, 16000–16007 (1996).
18. Parikh, S. S. *et al.* Base-excision repair initiation revealed by crystal structures and DNA-binding kinetics of human uracil-DNA glycosylase bound to DNA. *EMBO J.* **17**, 5214–5226 (1998).
19. Waters, T. R., Gallinari, P., Jiricny, J. & Swann, P. F. Human thymine DNA glycosylase binds to apurinic sites in DNA but is displaced by human apurinic endonuclease 1. *J. Biol. Chem.* **274**, 67–74 (1999).
20. Chen, D. S., Herman, V. & Demple, B. Two distinct human DNA diesterases that hydrolyze 3'-blocking deoxyribose fragments from oxidized DNA. *Nucleic Acids Res.* **19**, 5907–5914 (1991).
21. Horton, J. K., Srivastava, D. K., Zmudzka, B. Z. & Wilson, S. H. Strategic down-regulation of DNA polymerase beta by antisense RNA sensitizes mammalian cells to specific DNA damaging agents. *Nucleic Acids Res.* **23**, 3810–3815 (1995).
22. Kubota, Y. *et al.* Reconstitution of DNA base excision-repair with purified human proteins: interaction between DNA polymerase β and the XRCC1 protein. *EMBO J.* **15**, 6662–6670 (1996).
23. Caldecott, K. W., McKeown, C. K., Tucker, J. D., Ljungquist, S. & Thompson, L. H. An interaction between the mammalian DNA repair protein XRCC1 and DNA ligase III. *Mol. Cell. Biol.* **14**, 68–76 (1994).
24. Takeshita, M., Chang, C. N., Johnson, E., Will, S. & Grollman, A. P. Oligodeoxynucleotides containing synthetic abasic sites. Model substrates for DNA polymerases and apurinic/apyrimidinic endonucleases. *J. Biol. Chem.* **262**, 10171–10179 (1987).
25. Erzberger, J. P., Barsky, D., Scharer, O. D., Colvin, M. E. & Wilson, D. M. Elements in abasic site recognition by the major human and *Escherichia coli* apurinic/apyrimidinic endonucleases. *Nucleic Acids Res.* **26**, 2771–2778 (1998).
26. Otwinowski, Z. & Minor, W. Processing of X-ray diffraction data collected in oscillation mode. *Methods Enzymol.* **276**, 307–325 (1997).
27. Navaza, J. AMoRe: an automated package for molecular replacement. *Acta Crystallogr. A* **50**, 157–163 (1994).
28. Brünger, A. T., Kuriyan, J. & Karplus, M. Crystallographic R factor refinement by molecular dynamics. *Science* **235**, 458–460 (1987).
29. Read, R. J. Improved Fourier coefficients for maps using phases from partial structures with errors. *Acta Crystallogr. A* **42**, 140–149 (1986).
30. McRee, D. E. XtalView/Xfit—a versatile program for manipulating atomic coordinates and electron density. *J. Struct. Biol.* **125**, 156–165 (1999).

Supplementary information is available on Nature's World-Wide Web site (<http://www.nature.com>).

Acknowledgements

We thank S. S. Parikh, C. D. Putnam, D. S. Daniels and D. J. Hosfield for helpful discussions, and the staff and facilities at SSRL. This work was supported by the NIH, by a Laboratory Directed Research and Development grant from the Lawrence Berkeley Laboratory, by a cancer research supplement administered through LBNL from the National Cancer Institute (to J.A.T., S.M. and P. Cooper), the Skaggs Institute for Chemical Biology and a Special Fellowship from the Leukemia Society of America (to C.D.M.).

Correspondence and requests for materials should be addressed to J.A.T. (e-mail: jat@scripps.edu). Coordinates have been deposited in the RCSB Protein Data Bank under accession codes 1DE8, 1DE9 and 1DEW.

Design of single-layer β -sheets without a hydrophobic core

Shohei Koide*, Xiaolin Huang*, Karl Link*, Akiko Koide*, Zimei Bu† & Donald M. Engelman†

* Department of Biochemistry and Biophysics, University of Rochester Medical Center, Rochester, New York 14642, USA

† Department of Molecular Biophysics and Biochemistry, Yale University, New Haven, Connecticut 06511, USA

The hydrophobic effect is the main thermodynamic driving force in the folding of water-soluble proteins^{1,2}. Exclusion of nonpolar moieties from aqueous solvent results in the formation of a hydrophobic core in a protein, which has been generally considered essential for specifying and stabilizing the folded structures of proteins^{1–6}. Outer surface protein A (OspA) from *Borrelia*

burgdorferi contains a three-stranded β -sheet segment which connects two globular domains⁷. Although this single-layer β -sheet segment is exposed to solvent on both faces and thus does not contain a hydrophobic core, the segment has a high conformational stability⁸. Here we report the engineering of OspA variants that contain larger single-layer β -sheets (comprising five and seven β -strands) by duplicating a β -hairpin unit within the β -sheet. Nuclear magnetic resonance and small-angle X-ray scattering analyses reveal that these extended single-layer β -sheets are formed as designed, and amide hydrogen-deuterium exchange and chemical denaturation show that they are stable. Thus, interactions within the β -hairpin unit and those between adjacent units, which do not involve the formation of a hydrophobic core, are sufficient to specify and stabilize the single-layer β -sheet structure. Our results provide an expanded view of protein folding, misfolding and design.

The crystal structure of OspA revealed that this protein has an unusual architecture⁷: it is dumbbell-shaped and contains a three-stranded 'single-layer' β -sheet in the centre (Fig. 1). The single-layer β -sheet segment is rich in polar amino acids, and its amino-acid sequence does not follow the canonical, alternating hydrophobic/hydrophilic pattern usually found in amphipathic β -sheets (Fig. 2). Our previous studies showed that the solution structure of OspA is similar to the crystal structure^{9,10}, and that the protein, including the unusual single-layer β -sheet region, is highly stable^{8,11}.

The OspA single-layer β -sheet, although it does not contain a hydrophobic core, buries nonpolar surfaces to a degree comparable to that found in small globular proteins that do contain a hydrophobic core⁸. We attributed this effective burial of nonpolar surfaces to strategically placed amino acids with long side chains in the β -sheet. Despite the lack of a hydrophobic core in this region, the single-layer β -sheet architecture can gain sufficient stabilization from the hydrophobic effect, generally considered the dominant factor in protein stability^{1,2}. However, β -strands 8 and 10 of the three-stranded single-layer β -sheet make extensive interactions with the globular domains (Fig. 1), and thus these two strands

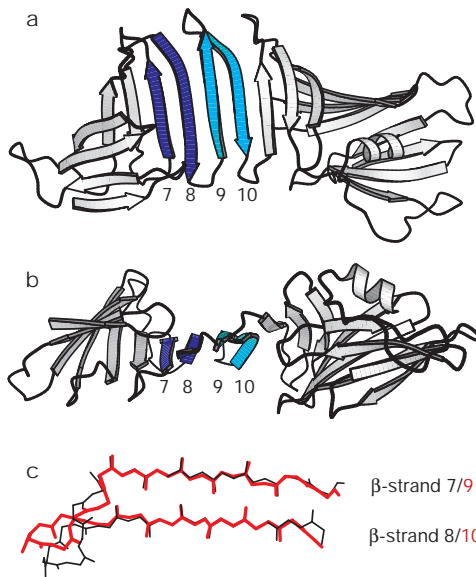


Figure 1 Structure of wild-type OspA. **a, b**, Drawings of the OspA structure⁷. The molecule in **b** is rotated along a horizontal axis relative to the molecule in **a**. The homologous β -hairpins (β -strands 7 and 8, and 9 and 10) in the single-layer β -sheet region are labelled and shown in blue and cyan, respectively. **c**, Superposition of the β -hairpin units. β -strands 7 and 8 (residues 95–118; black lines) and 9 and 10 (119–141; red lines) have been superimposed using C α atoms in the β -strand regions. The root-mean-squared deviation for the backbone atoms in the β -strands is 0.51 Å.

could be considered as edge strands of the two globular domains. There are also a few interactions between the ninth, central, strand and the globular domains⁷. Thus, it could not be excluded that the single-layer β -sheet region is stably held only because it is a short segment tightly packed between two globular domains. Here, we examined whether interactions within the single-layer β -sheet region are sufficient to specify and sustain the β -sheet structure, by designing extended single-layer β -sheets and characterizing their structure and stability.

Two β -hairpins in and adjacent to the single-layer β -sheet region (β -strands 7 and 8, and 9 and 10, respectively) have homologous amino-acid sequences (Fig. 2), and their conformations are similar (Fig. 1c). This suggests that a β -hairpin unit similar to the existing ones could be inserted between β -strands 8 and 9, which would reproduce most of the original interstrand interactions (Fig. 2). Thus, we engineered OspA variants in which a β -hairpin segment (residues 119–141) was duplicated and triplicated (called OspA+1bh and OspA+2bh, respectively; Fig. 2).

We have completed the backbone NMR assignments of OspA+1bh (280 residues). Carbon-13 NMR chemical shifts of the C_{α} and C_{β} atoms are sensitive to the peptide backbone configuration, and thus they are accurate measures for identifying secondary structure elements¹². An analysis of ¹³C chemical shifts of OspA+1bh revealed that the inserted segment (residues 119'–141') contains two β -strands as designed (Fig. 3b, c). The chemical-shift profiles of the two original β -hairpin units (β -strands 7 and 8, and 9 and 10) show only small changes upon the β -hairpin insertion in OspA+1bh (Fig. 3b, c). The chemical-shift profile of the inserted segment (strands 9' and 10') closely resembles that of strands 9 and 10. These results indicate that the conformation of the inserted segment may be similar to that of β -strands 9 and 10, and that the insertion did not significantly affect the conformations of the original β -strands (7, 8, 9 and 10) of the β -sheet. Furthermore, characteristic nuclear Overhauser effect (NOE) connectivities were detected in and near the insertion (Fig. 2), showing that the peptide backbone of the extended single-layer β -sheet is folded as designed. Residues in the globular domains of OspA+1bh show small or no chemical-shift deviations from those of wild-type OspA (data not shown), indicating small effects of the β -hairpin insertion on the globular domains. ¹H–¹⁵N NOE measurements provide information on the conformational dynamics of individual amide N–H bond vectors¹³. In OspA+1bh, residues that have reduced ¹H–¹⁵N NOE are localized in the terminal and loop regions, and the residues in the β -strands of the extended single-layer β -sheet have ¹H–¹⁵N NOEs close to the average (Fig. 3d), indicating that the region is not highly mobile on a picosecond–nanosecond timescale.

The ratio of the ¹⁵N longitudinal and transverse relaxation times

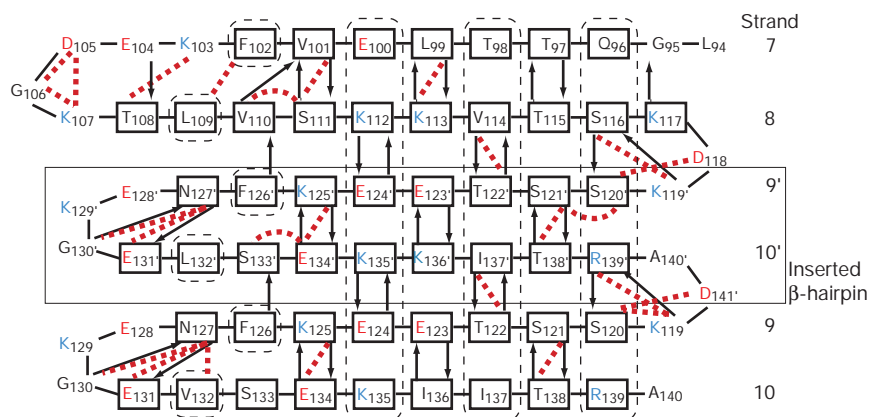


Figure 2 The β -sheet extension design in OspA+1bh. Residues 119'–141' denote those in the insertion. Two conservative mutations at residues 132' and 136' were introduced in the new β -hairpin to reduce the sequence identity between the β -strands 9'–10' and 9–10, and hence to increase the dispersion of NMR spectra. Residues in boxes are those

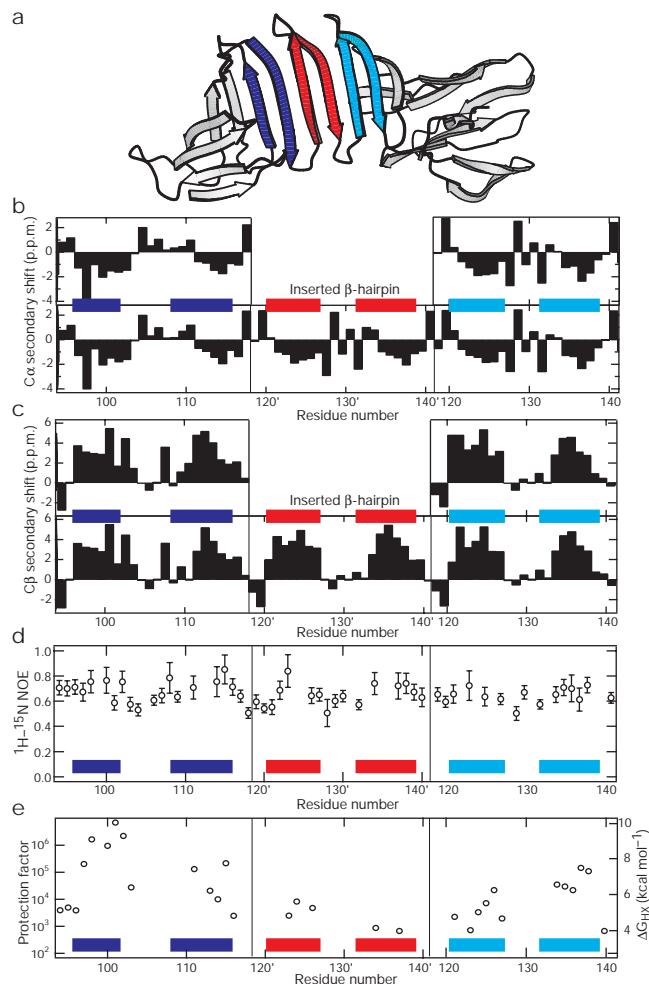


Figure 3 NMR characterization of the extended single-layer β -sheet in OspA+1bh. **a**, The model structure of OspA+1bh. **b, c**, Secondary shifts¹² of ¹³C _{α} (**b**) and ¹³C _{β} (**c**) plotted against residue number. Consecutive residues with a ¹³C _{α} secondary shift larger than 0.7 p.p.m. with a ¹³C _{β} secondary shift smaller than –0.7 p.p.m. define a β -strand¹². Upper rows show data for wild-type OspA, and the lower rows for OspA+1bh. Residue numbering is according to that in Fig. 2. Horizontal bars indicate the locations of predicted β -strands in OspA+1bh, and those of β -strands in the wild-type OspA crystal structure. **d**, ¹H–¹⁵N NOE intensities plotted against residue number. **e**, Amide HX protection factors¹⁸ ($P = k_{\text{intrinsic}}/k_{\text{observed}}$, where $k_{\text{intrinsic}}$ is the reference HX rate in the unstructured peptide; the scale is shown on the left vertical axis) plotted against residue number. The scale for the free energy of opening of a hydrogen-bonded amide proton ($\Delta G_{\text{HX}} = RT \ln(P)$) is shown on the right vertical axis.

within β -strands; residues in dashed lines have side chains protruding toward the reader. Hydrogen bonds are shown as arrows, with the arrowhead pointing to the carbonyl group. Unambiguously observed H^N–H^N NOEs are shown as red dashed lines.

(T_1 and T_2 , respectively) is a good measure for the rate at which each N–H bond vector reorients because of global tumbling¹³, and it can be used to define long-range order in a protein that has a significant rotational diffusion anisotropy¹⁴. The ^{15}N T_1/T_2 ratios for 108 residues in OspA+1bh range from 14 to 50 (Fig. 4), indicating a large rotational diffusion anisotropy of the molecule. The data were best fitted with the equation describing the theoretical dependence of the T_1/T_2 ratio on the angle θ between the N–H bond vector and the long axis of the rotational diffusion tensor, when the diffusion axis is aligned parallel to the unique axis of the inertia tensor of the model structure (Fig. 4)^{10,14,15}. Data for residues from the amino- and carboxy-terminal globular domains have similar dependence on θ (Fig. 4), showing that the whole OspA+1bh molecule tumbles as a fairly rigid entity. Furthermore, many of the residues located in the β -strands of the single-layer β -sheet have large ^{15}N T_1/T_2 ratios that indicate slow tumbling. This is consistent with the model structure, in which the N–H bond vectors of these residues have small angles with the long axis of the molecule (Figs 2 and 3a).

Small-angle X-ray scattering (SAXS) has proved to be useful in defining the global conformation of a nonspherical molecule, such as OspA (ref. 9), and in distinguishing compact denatured states from a native protein¹⁶. The radius of gyration (R_g) for OspA+1bh was determined to be $28.4 \pm 0.2 \text{ \AA}$, in an excellent agreement with an estimated value of $28.5 \pm 0.1 \text{ \AA}$ from the model structure (Figs 3a and 5a). A radial Patterson ($P(r)$) curve, which is a real-space representation of the information in a scattering curve, shows the length distribution of atom-weighted interatomic vectors in the particle¹⁷. The $P(r)$ curve for OspA+1bh agrees well with that predicted from a model structure (Fig. 5a). In contrast, the $P(r)$ curve for a structural ensemble, in which the inserted segment is assumed to be a flexible linker, is distinct from the experimental data. Taken together, our NMR and SAXS data of OspA+1bh show that the extended single-layer β -sheet is formed as designed, that OspA+1bh is predominantly monomeric in solution, and that the insertion of the β -hairpin does not cause a significant bending of the β -sheet.

The R_g of OspA+2bh, the protein with two β -hairpin inserts, was determined to be $30.7 \pm 0.6 \text{ \AA}$, which is in good agreement with an estimation of $31.4 \pm 0.1 \text{ \AA}$ from our model. Its $P(r)$ curve also

agrees well with the prediction (Fig. 5b). We have not completed NMR characterization of OspA+2bh, because of technical difficulties associated with the larger molecular weight and the repetitive sequence in the single-layer β -sheet; however, the SAXS data indicate that the seven-stranded single-layer β -sheet may also fold into the designed structure. This is a critical test of the design, as the insertion of the second β -hairpin unit into the β -sheet of OspA+1bh should reproduce most of the interactions between the β -hairpin units that are already present in OspA+1bh (Fig. 2).

The degree of protection of amide protons from solvent exchange distinguishes a tightly packed protein from a loosely packed, molten-globule-like state^{3,18,19}. Amide hydrogen–deuterium exchange (HX) rates were determined for 117 amide protons of OspA+1bh at 45°C and pH 6.09. Each of the five β -strands of the extended single-layer β -sheet contains amide protons that exhibit substantial protection (Fig. 3e). Similar to the wild-type protein⁸, the most protected amides are located in the N-terminal globular domain. The free energies of ‘opening’ hydrogen bonds for the protected amides in strands 8, 9', 10', 9 and 10 range from 4.1 to $7.7 \text{ kcal mol}^{-1}$ at 45°C , indicating that the extended single-layer β -sheet is tightly packed. The relatively low protection factors for β -strands 9' and 10' indicate an increased mobility of the region. This might be due to suboptimum packing of the inserted segment caused by the two mutations at residues 132' and 136' (Fig. 2).

OspA undergoes a twostep unfolding reaction, in which the C-terminal folding unit, including β -strand 9 to the C terminus, unfolds first¹¹. Thus, the boundary between the two folding units coincides with that between the two homologous β -hairpins in the single-layer β -sheet (Fig. 2). Stability of the C-terminal unit can be specifically determined using fluorescence emission of the single tryptophan residue in this unit¹¹. A mutation in β -strand 9, F126A, decreases the unfolding free energy of the C-terminal folding unit by $2.0 \text{ kcal mol}^{-1}$ (Fig. 6), indicating that the stability of the OspA C-terminal folding unit is sensitive to perturbation in the single-layer β -sheet. Consequently, the stability measurement of the C-terminal folding unit can be used to probe the integrity of the single-layer β -sheet. The unfolding free energies of the C-terminal folding unit in the wild-type protein, OspA+1bh and OspA+2bh are $8.3 (\pm 0.2)$, $9.2 (\pm 0.2)$ and $8.8 (\pm 0.3) \text{ kcal mol}^{-1}$, respectively. The similar

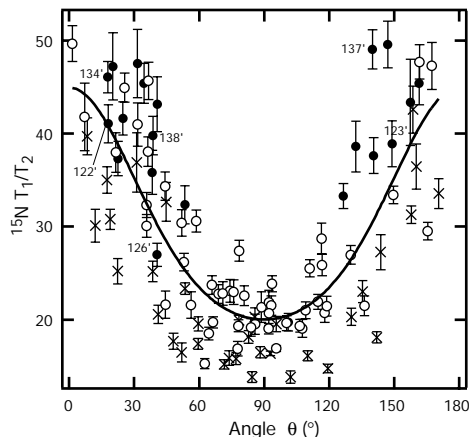


Figure 4 Nitrogen-15 T_1/T_2 ratios of the amide ^{15}N nuclei in OspA+1bh plotted against the angle θ between the N–H bond vectors and the estimated unique axis of the rotational diffusion tensor. Crosses indicate data for residues in the N-terminal globular domain, filled circles for those in the single-layer β -sheet, and open circles for those in the C-terminal globular domain. Data for residues in the inserted β -hairpin are labelled with residue numbers. The curve shows the best fit of the equation describing the θ dependence of the T_1/T_2 ratio^{14,15}.

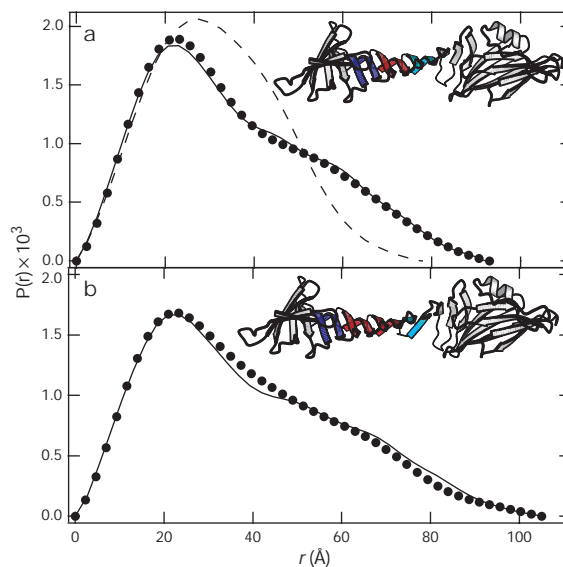


Figure 5 The $P(r)$ functions of OspA+1bh (a) and OspA+2bh (b) determined from SAXS data. Circles show experimental data, and the continuous lines are predictions from the models. In a, the broken line shows the $P(r)$ function for a structural model in which the inserted segment is assumed to be flexible. Models of the two proteins are also shown with the inserted β -hairpins in red.

stabilities for the three proteins show that the integrity of the single-layer β -sheet is maintained in the extended β -sheets. In contrast, an OspA+1bh variant containing three mutations in the inserted β -hairpin (K119'T/F126'L/K135'G) has a markedly reduced stability ($\Delta\Delta G^0 = 3.1 \text{ kcal mol}^{-1}$; Fig. 6), further confirming that the segment is an integral part of the protein. The dependence of the unfolding free energy on denaturant concentration (the m -value) was $2.44 (\pm 0.07)$, $2.88 (\pm 0.08)$ and $3.09 (\pm 0.11)$ for OspA, OspA+1bh and OspA+2bh, respectively. The m -value is known to correlate well with the change in solvent-accessible surface area upon unfolding²⁰; thus, the incremental increase in the m -value for OspA+1bh and OspA+2bh compared with that of the wild-type suggests that the size of the C-terminal folding unit increases as more β -hairpins are incorporated in the single-layer β -sheet, and that the insertion is part of the C-terminal folding unit.

Our successful design of large, stable single-layer β -sheets is, to our knowledge, the first example of the stable extension of a β -sheet in a natural protein. Further extension of the OspA β -sheet should be quite feasible, as no significant decrease in conformational stability occurred in OspA+1bh and OspA+2bh. Our results clearly indicate that interactions within the β -hairpin units, and between adjacent units, are sufficient for stability within the extended single-layer β -sheet structure. Thus, our results indicate that it may be possible to design a stable protein without the formation of a hydrophobic core. Peptides that form three-stranded β -sheets have been successfully designed²¹; also, the WW domain has been shown to fold as a three-stranded β -sheet^{22,23}. The high stabilities of the single-layer β -sheets in OspA variants are distinct from the marginal stabilities observed for these three-stranded β -sheets. This difference can be attributed to the fact that both edges of the OspA single-layer β -sheets are capped with globular domains that sequester additional surface areas of the single-layer β -sheet⁸. Thus, effective burial of the edge-strand surfaces may be important for the design of a small β -sheet motif with a high stability.

It is tempting to speculate that single-layer β -sheet structures may be involved in increases of β -sheet content that are associated with amyloid-like fibril formation and protein aggregation^{24,25}, because a single-layer β -sheet could be formed with a segment of a protein possessing a hydrophobic periodicity compatible with an amphipathic α -helix; such a β -sheet does not require the alternating hydrophobic/hydrophilic pattern of the amphipathic β -sheet. We have proposed that amino acids with long side chains play important roles in stabilizing the single-layer β -sheet structure by burying nonpolar surfaces⁸. It is intriguing that the 'polar zipper' sequences identified by Perutz *et al.*²⁶, such as the poly-glutamines associated with Huntington's disease, appear to satisfy the proposed requirements of stable single-layer β -sheets, suggesting potential involvement of single-layer β -sheet structures in human diseases.

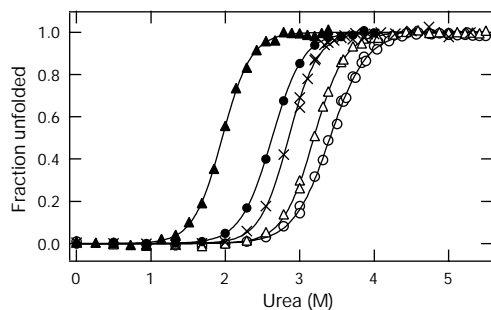


Figure 6 Urea-induced unfolding of wild-type OspA (open circles), OspA+1bh (open triangles), OspA+2bh (crosses), OspA mutant F126A (filled circles) and OspA+1bh mutant K119'T/F126'L/K135'G (closed triangles). Urea-induced unfolding reactions of the C-terminal folding unit in these proteins were followed using fluorescence emission from the single tryptophan residue in the C-terminal globular domain¹¹. The data were converted to fraction unfolded, according to the standard two-state model¹¹.

Methods

Sample preparation

The gene for OspA+1bh was constructed by inserting a 69-base pair (bp) DNA segment coding for the β -hairpin sequence (Fig. 2) in the wild-type OspA gene, using standard polymerase chain reaction (PCR) techniques. The second insertion was made by ligating a 69-bp DNA duplex at a unique restriction site (*Bse*RI) within the first insert. The F126A mutation was introduced using standard oligonucleotide-directed mutagenesis. Two unplanned mutations, K119'T and F126'L, were introduced by PCR errors during the construction of an OspA+1bh mutant, K135'G, which resulted in the triple mutations. The entire genes were sequenced to confirm that no other mutations had been introduced. The proteins were expressed and purified as described¹⁰.

NMR spectroscopy

The NMR sample contained 1.3 mM ¹³C,¹⁵N-OspA+1bh in 10 mM sodium phosphate buffer, pH 6.0, with 50 mM sodium chloride in 95% H₂O and 5% D₂O. All NMR experiments were performed at 45 °C on a Varian Inova 600 spectrometer. Resonance assignments of OspA+1bh were achieved using standard triple resonance techniques, as described for wild-type OspA (ref. 10). H^N-H^N NOEs were identified in a 3D ¹⁵N-edited NOESY spectrum²⁷. The chemical-shift data have been deposited in the BioMagRes Bank (accession number 4367). Carbon-13 secondary chemical shifts were calculated as the differences from respective random-coil shifts¹². Amide HX measurements were performed on a 1.0 mM ¹⁵N-sample in sodium phosphate buffer (10 mM, pH* 6.09, the direct pH meter reading) containing sodium chloride (50 mM) at 45 °C, as described previously⁸. ¹H-¹⁵N NOE and ¹⁵N T₁ and T₂ values were measured using published procedures^{10,28}. The N-H bond vectors were calculated from an energy-minimized structural model of OspA+1bh, as described¹⁰. The rotation diffusion property of this model structure can be well described with an axially symmetric diffusion model, in which the molecule is approximated as a prolate ellipsoid. The dependence of the T₁/T₂ ratio on the angle between the N-H vector and the unique axis of the diffusion tensor was analysed according to this model^{10,15}.

Small-angle X-ray scattering

The proteins were dissolved in sodium phosphate buffer (10 mM, pH 6.0) containing sodium chloride (50 mM). The protein concentrations were 5.2 and 5.15 mg ml⁻¹, for OspA+1bh and OspA+2bh, respectively. SAXS experiments were carried out at 30 °C as described⁹. Forty structures of OspA+1bh, in which the N- and C-terminal fragments were linked with a flexible linker corresponding to the inserted segment, were calculated using simulated annealing²⁹ with distance restraints that maintained the conformations of the terminal fragments.

Urea denaturation

Experiments were carried out in 10 mM sodium phosphate buffer (pH 6.0) with 50 mM sodium chloride at 30 °C, as previously¹¹.

Molecular graphics

We used Quanta (Molecular Simulations) for molecular modelling. The structures of OspA+1bh and OspA+2bh were modelled, in which the single-layer β -sheet was extended with an assumption that the inserted β -hairpin takes on a conformation similar to that of β -strands 9 and 10. Drawings were made using MOLSCRIPT³⁰.

Received 12 August; accepted 1 November 1999.

- Kauzmann, W. Some factors in the interpretation of protein denaturation. *Adv. Prot. Chem.* **14**, 1–63 (1959).
- Dill, K. A. Dominant forces in protein folding. *Biochemistry* **29**, 7133–7155 (1990).
- Harbury, P. B., Plecs, J. J., Tidor, B., Alber, T. & Kim, P. S. High-resolution protein design with backbone freedom. *Science* **282**, 1462–1467 (1998).
- Beasley, J. R. & Hecht, M. H. Protein design: the choice of de novo sequences. *J. Biol. Chem.* **272**, 2031–2034 (1997).
- Bryson, J. W. *et al.* Protein design: a hierarchic approach. *Science* **270**, 935–941 (1995).
- Dahiyat, B. I. & Mayo, S. L. De novo protein design: fully automated sequence selection. *Science* **278**, 82–87 (1997).
- Li, H., Dunn, J. J., Luft, B. J. & Lawson, C. L. Crystal structure of Lyme disease antigen outer surface protein A complexed with an Fab. *Proc. Natl Acad. Sci. USA* **94**, 3584–3589 (1997).
- Pham, T.-N., Koide, A. & Koide, S. A stable single-layer β -sheet without a hydrophobic core. *Nature Struct. Biol.* **5**, 115–119 (1998).
- Bu, Z., Koide, S. & Engelman, D. M. A solution SAXS study of *Borrelia burgdorferi* OspA, a protein containing a single-layer β -sheet. *Protein Sci.* **7**, 2681–2683 (1998).
- Pham, T. N. & Koide, S. NMR studies of *Borrelia burgdorferi* OspA, a 28 kDa protein containing a single-layer β -sheet. *J. Biomol. NMR* **11**, 407–414 (1998).
- Koide, S. *et al.* Multi-step denaturation of *Borrelia burgdorferi* OspA, a protein containing a single-layer β -sheet. *Biochemistry* **38**, 4757–4767 (1999).
- Wishart, D. S. & Sykes, B. D. The ¹³C chemical-shift index: a simple method for the identification of protein secondary structure using ¹³C chemical-shift data. *J. Biomol. NMR* **4**, 171–180 (1994).
- Kay, L. E., Torchia, D. A. & Bax, A. Backbone dynamics of proteins as studied by ¹⁵N inverse detected heteronuclear NMR spectroscopy: application to staphylococcal nuclease. *Biochemistry* **28**, 8972–8979 (1989).
- Tjandra, N., Garrett, D. S., Gronenborn, A. M., Bax, A. & Clore, G. M. Defining long range order in NMR structure determination from the dependence of heteronuclear relaxation times on rotational diffusion anisotropy. *Nature Struct. Biol.* **4**, 443–449 (1997).

15. Lee, L. K., Rance, M., Chazin, W. J. & Palmer, A. G. Rotational diffusion anisotropy of proteins from simultaneous analysis of ^{15}N and $^{13}\text{C}\alpha$ nuclear spin relaxation. *J. Biomol. NMR* **9**, 287–298 (1997).
16. Kataoka, M., Kuwajima, K., Tokunaga, F. & Goto, Y. Structural characterization of the molten globule of alpha-lactalbumin by solution X-ray scattering. *Protein Sci.* **6**, 422–430 (1997).
17. Lattman, E. E. Small angle scattering studies of protein folding. *Curr. Opin. Struct. Biol.* **4**, 87–92 (1994).
18. Englander, S. W. & Kallenbach, N. R. Hydrogen exchange and structural dynamics of proteins and nucleic acids. *Q. Rev. Biophys.* **6**, 521–655 (1984).
19. Hughson, F. M., Wright, P. E. & Baldwin, R. L. Structural characterization of a partly folded apomyoglobin intermediate. *Science* **249**, 1544–1548 (1990).
20. Myers, J. K., Pace, C. N. & Scholtz, J. M. Denaturant m values and heat capacity changes: relation to changes in accessible surface areas of protein unfolding. *Protein Sci.* **4**, 2138–2148 (1995).
21. Lacroix, E., Kortemme, T., de la Paz, M. L. & Serrano, L. The design of linear peptides that fold as monomeric beta-sheet structures. *Curr. Opin. Struct. Biol.* **9**, 487–493 (1999).
22. Macias, M. J. *et al.* Structure of the WW domain of a kinase-associated protein complexed with a proline-rich peptide. *Nature* **382**, 646–649 (1996).
23. Koepf, E. K., Petrassi, H. M., Sudol, M. & Kelly, J. W. WW: An isolated three-stranded antiparallel beta-sheet domain that unfolds and refolds reversibly; evidence for a structured hydrophobic cluster in urea and GdnHCl and a disordered thermal unfolded state. *Protein Sci.* **8**, 841–853 (1999).
24. Fink, A. L. Protein aggregation: folding aggregates, inclusion bodies and amyloid. *Fold. Des.* **3**, R9–R23 (1998).
25. Kelly, J. W. The alternative conformations of amyloidogenic proteins and their multi-step assembly pathways. *Curr. Opin. Struct. Biol.* **8**, 101–106 (1998).
26. Perutz, M. F., Johnson, T., Suzuki, M. & Finch, J. T. Glutamine repeats as polar zippers: their possible role in inherited neurodegenerative diseases. *Proc. Natl Acad. Sci. USA* **91**, 5355–5358 (1994).
27. Clore, G. M. & Gronenborn, A. M. Applications of three- and four-dimensional heteronuclear NMR spectroscopy to protein structure determination. *Prog. NMR Spectrosc.* **23**, 43–92 (1991).
28. Farrow, N. A. *et al.* Backbone dynamics of a free and phosphopeptide-complexed Src homology 2 domain studied by ^{15}N NMR relaxation. *Biochemistry* **33**, 5984–6003 (1994).
29. Brunger, A. T. *et al.* Crystallography & NMR system: a new software suite for macromolecular structure determination. *Acta Crystallogr. D* **54**, 905–921 (1998).
30. Kraulis, P. MOLSCRIPT: a program to produce both detailed and schematic plots of protein structures. *J. Appl. Cryst.* **24**, 946–950 (1991).

Acknowledgements

We thank B. M. Goldstein and J. J. Hayes for discussions; F. Delaglio, B. Johnson, L. E. Kay and A. G. Palmer III for NMR programs; and S. D. Kennedy for technical support. This work was supported in part by NIH grants to S.K. and D.M.E.

Correspondence and requests for materials should be addressed to S.K. (e-mail: Shohei_Koide@urmc.rochester.edu).